LAWRENCE LIVERMORE NATIONAL LABORATORY

LLNL-TR-718138

Analyses of Field Test Data at the Atucha-1 Spent Fuel Pools

S. Sitaraman

January 17, 2017

This work performed under the auspices of the U.S. Department of Energy by Lawrence Livermore National Laboratory under Contract DE-AC52-07NA27344.

Analyses of Field Test Data at the Atucha-1 Spent Fuel Pools

Shivakumar Sitaraman
Lawrence Livermore National Laboratory
Email: sitaraman1@llnl.gov

Executive Summary

A field test was conducted at the Atucha-1 spent nuclear fuel pools to validate a software package for gross defect detection that is used in conjunction with the inspection tool, Spent Fuel Neutron Counter (SFNC). A set of measurements was taken with the SFNC and the software predictions were compared with these data and analyzed. The data spanned a wide range of cooling times and a set of burnup levels leading to count rates from the several hundreds to around twenty per second. The current calibration in the software using linear fitting required the use of multiple calibration factors to cover the entire range of count rates recorded. The solution to this was to use power regression data fitting to normalize the predicted response and derive one calibration factor that can be applied to the entire set of data. The resulting comparisons between the predicted and measured responses were generally good and provided a quantitative method of detecting missing fuel in virtually all situations. Since the current version of the software uses the linear calibration method, it would need to be updated with the new power regression method to make it more user-friendly for real time verification and fieldable for the range of responses that will be encountered.

Introduction

The objective of the Atucha-1 field test exercise was to deploy the SFNC to measure gross neutron signals and couple it with the Spent Fuel Verification Tool, a software package designed for predictive gross defect detection at the site. The exercise was to test the capability of the existing algorithm in the software to predict the neutron signal at the measurement locations and determine if any updates to the software are needed to make it an effective gross defect verification tool.

A set of measurements was taken at spent fuel pools located at the Central Nuclear Juan Domingo Peron Atucha-1 nuclear site during the week of October 24-28, 2016. The measured data were entered manually into the software, and compared to a predicted response to verify the presence of the fuel within a certain tolerance set by the user. The main set of measurements was taken in Pool 4 followed by a few in Pools 5 and 6. The contents of Pool 7 had not changed since the previous measurement campaign in early 2004. However, only a small section of the pool was accessible for measurements and a few readings were available for comparison with the 2004 data. All measurements were taken in the upper layer of the pools during this field test exercise. The following sections will present the analyses of the data acquired from all the pools.

Spent Fuel Neutron Counter

The SFNC uses a fission chamber to collect the gross neutron signal and has an active length of 127mm and an outer diameter of 25mm. It is surrounded by a 9.5-mm thick polyethylene sheath that serves as a moderator. The fission chamber is connected to the pre-amplifier which in turn is connected via standard IAEA yellow 30m cable to a mini multichannel analyzer and a laptop. The SFNC is enclosed in stainless steel and has a total length of 285mm and a diameter of 56mm. Figure 1 shows a schematic of the system. The SFNC is inserted into the gap formed by four adjacent spent fuel assemblies (SFA) and a removable collar is used to center the system in the gap.

The specific system used had a fission chamber with the ID FC 9817/055 and was the same system used in an earlier measurement campaign conducted in 2004. It showed good stability in an environment with gross neutron signals ranging from over 800 cps to 20 cps encompassing various burnups and cooling times present in the various pools. The pre-amplifier used was a PDT10A-HN with serial number 0317508.

The measurements were performed with the help of a movable bracket that was fixed to the guard rails of the crane and provided sufficient clearance from the crane for the SFNC to be safely lowered into the pool using the cable. After an initial determination of the axial level of the peak signal, all measurements were made at that axial level. It is a good practice to repeat this exercise when the tool is deployed next to determine the axial level where the peak response occurs. The measurement time was 60 seconds and the typical time between successive measurements was about 5 minutes.

Spent Fuel Verification Tool

The software, Spent Fuel Verification Tool, was developed on a LabVIEW platform that is available from National Instruments (NI). To run the software, the user needs only a runtime executable that can be directly downloaded from the NI website. The basic algorithm consists of a set of transfer functions in a 47-energy neutron group structure based on the inter-assembly pitch that is used to suspend the assemblies from the hangers (known as *perchas)* in the pools. There are three pitches present in the pools-150mm x 150mm, 123mm x 135mm, and 123mm x 150mm. The software database also contains source terms based on both cooling time and burnup for each of the two initial enrichments – natural and slightly enriched to 0.85% U235. These source spectra are in the identical 47-group energy structure. Interpolation in cooling time and burnup will result in the correct source spectrum that the appropriate transfer function is folded into and summed over all groups to produce a signal at the detector consistent with the spent fuel assembly's properties. In addition to the four adjacent assemblies, an additional 32 assemblies in the vicinity are also considered for their contribution to the signal at the detector. Detailed descriptions of the functioning of the software can be found in references 1 and 2. The total contribution from all 36 assemblies gives the predicted response. To account for the detector efficiency, these signals need to be calibrated against a set of measured signals using an appropriate regression technique. The current version of the software uses a linear least squares estimate to produce a calibration factor that is applied to the predicted response in order for it to be compared to the measured signal. A default tolerance value of 15% is set in the software to account for various uncertainties inherent in the methodology [1]. This can be reset by the user and any comparisons between prediction and measurement within the set tolerance is considered to be acceptable.

Figure 1. Spent Fuel Neutron Counter

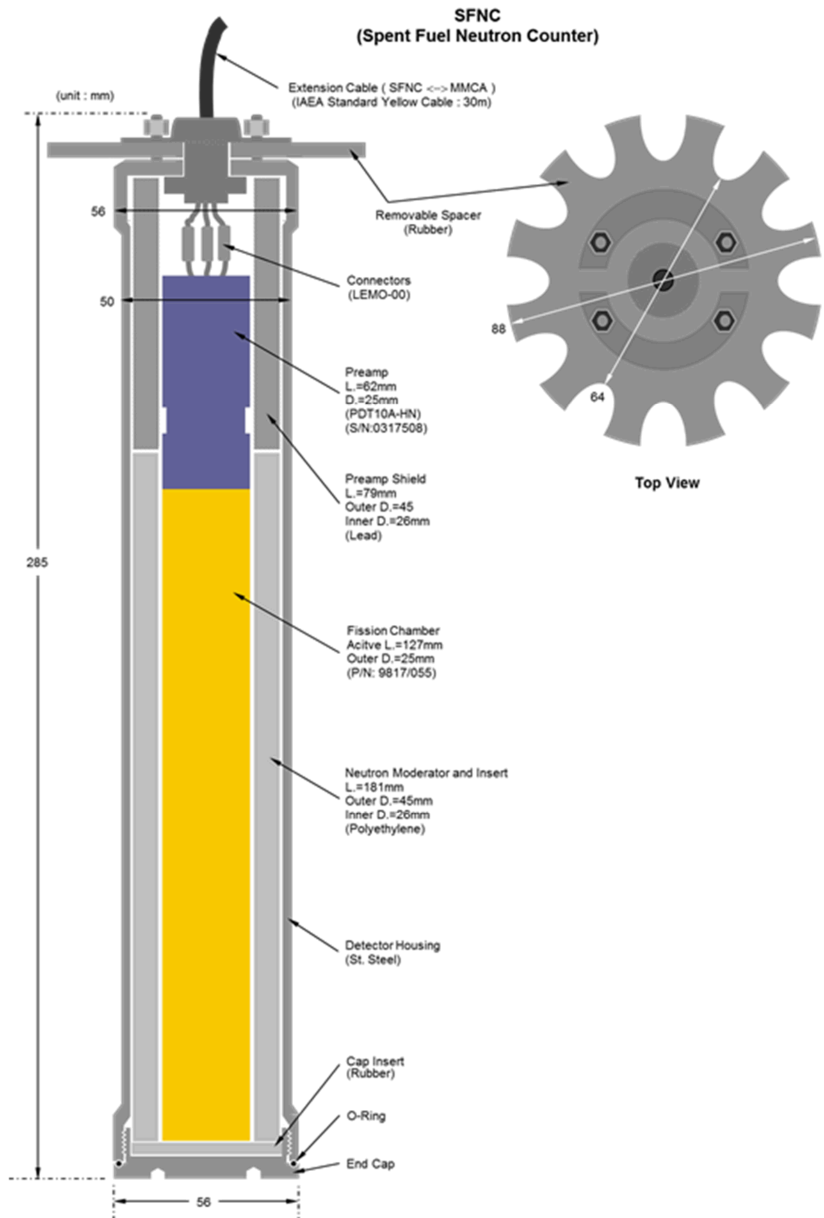

General Observations of the Spent Fuel

Atucha-1 operated for several years with natural uranium (NU) fuel and typical discharge burnup levels were in the range of 5500 to 7000 MWd/t. Since 2001, the initial enrichment of the fuel being loaded into the core was raised to a slightly enriched level of 0.85% in U-235 (SEU). This lead to discharged fuel with high burnup levels of 10,000 to 12,000 MWd/t. Measurements were conducted during this field test mainly in Pool 4 that consisted of principally SEU fuel. Thus, most of the spent fuel assemblies (SFAs) in the upper level, where all the measurements were performed, had high burnup levels. In addition, this batch of SFAs had cooling times ranging from a few months to over 15 years. There were seven old NU assemblies out of the total of 1004 SFAs at this level with long cooling times. A total of 32 individual measurements were made spanning this range of cooling times. In the earlier 2004 measurement campaign [2], the upper level of pool 4 consisted of NU fuel with low burnups and very large cooling times leading to count rates well below 100 cps. Count rates in the upper level of pools 5 and 6 had a mix of NU and SEU fuel with cooling times of generally over 15 years or between 2 and 15 years. In these two pools, measurements were made at locations where the adjacent four assemblies were a mix of NU and SEU spent fuel. Only four measurements were made in Pool 7 due to accessibility issues. These SFAs in the upper level of this pool were undisturbed since the last set of measurements was taken in 2004. Thus, comparisons between the current and previous data could be made to determine the level of decrease in count rates after an additional 12.5 years of cooling time. In summary, the data set provided a large range of count rates from 20 cps to close to 900 cps in the fifty-six unique measurements performed. This is in contrast to the large set of data from the 2004 campaign that was predominantly in the less than 50 cps range.

The software reads a master file provided by the operator containing all the properties of the SFAs and their positions in the pool. The user can use the software to examine all the properties of every SFA in the vicinity of the locations chosen for performing measurements. As mentioned earlier, the SFAs stored in the various pools have essentially two burn up ranges: 5500-7000 MWd/t for NU fuel and 10,000 to 12000 MWd/t for the SEU fuel. Currently, only SEU fuel is being used and consequently future SFAs discharged into the pools will be in the high burnup range. Cooling times for the discharged SEU fuel will range from newly discharged to much longer cooling times well beyond 15 years. Since no NU SFAs are now being discharged, those present in the pools will continue to age over time and produce very low count rates. The user can examine the layout in terms of both burn up and cooling time and determine a good mix of these factors to ensure an appropriate range of count rates will be recorded from the standpoint of calibrating the software. As described in reference 2, the calibration factors can be re-used unless a long time has elapsed between measurement exercises or the instrumentation in the tool has been replaced.

Analyses of the Field Test Data

The current algorithm in the software uses linear regression to calibrate it against a set of measurements. The large range in the recorded count rates required the use of multiple linear calibrations resulting in the user having to apply different calibration factors for different ranges of count rates in order for the predicted response to be consistent with the measured response within the tolerance value of 15%. This would clearly not be a user-friendly situation with the user potentially having to open multiple software windows each with its own linear calibration set based on the different ranges of count rates, to have real time information for verification of the presence of the surrounding SFAs.

Upon comparison of the fifty-six uncalibrated predicted responses from the software and the corresponding measurements, it became clear that a more appropriate method for calibration would be to use power law regression. Since this feature does not exist in the current version of the software, this was derived by hand and applied to the data using spreadsheets.

The resulting fit takes the following form: $y = \mathrm{A}x^{B}$,

Where y is the measured response, x is the uncalibrated predicted response and A and B are constants.

This scheme worked well with requiring only one value of A and B to provide a good fit to the measured data. Fifteen out of the fifty-six data points, shown in Table 1, spanning a range of count rates from 22 cps to 778 cps were used to calculate the calibration factors A and B. These were selected so that they represented approximately 50 cps increments. Using this set results in A=2.029e-10±1.07e-10 and B=1.459±0.028 with a correlation of 0.998. The uncertainty in the difference between measured and predicted was estimated to be approximately 15%. These values were then used to calibrate the predicted responses for the fifty-six cases for comparison with the measured responses.

Table 1. Calibration Data

Measured Data	Uncalibrated Prediction
21.62	3.72E+07
31.82	4.42E+07
51.30	6.32E+07
102.97	1.05E+08
144.68	1.39E+08
193.68	1.85E+08
220.48	1.76E+08
260.25	2.07E+08
299.23	2.26E+08
348.93	2.40E+08
403.33	2.64E+08
480.82	2.78E+08
530.10	3.23E+08
715.27	3.97E+08
777.67	4.02E+08

Table 2 presents the comparisons of the predicted and measured responses using the new power regression calibration as well as the comparisons of the data using a single linear regression calibration factor based on the points presented in Table 1.

Table 2. Comparison of Predicted and Measured Response

Position row	Position Column	Measured	Power Regression			Linear Regression	
			Predicted	Percent Difference ±uncertainty		Predicted	Percent Difference
44:45	N:O	366.00	313.21	16.86%	2.53%	362.41	0.99%
44:45	K:L	299.23	313.21	-4.46%	0.67%	362.41	-17.43%
43:44	K:L	254.48	270.08	-5.78%	0.87%	327.42	-22.28%
38:39	H:J	294.25	286.46	2.72%	0.41%	340.90	-13.68%
38:39	Q:R	353.53	292.18	21.00%	3.15%	345.56	2.31%

38:39	Z1:Z2	276.88	260.10	6.45%	0.97%	319.07	-13.22%
44:45	X:Y	260.25	276.67	-5.94%	0.89%	332.88	-21.82%
51:52	V:W	348.93	341.94	2.04%	0.31%	384.88	-9.34%
51:52	K:L	385.32	386.71	-0.36%	0.05%	418.74	-7.98%
57:58	H:J	480.82	425.13	13.10%	1.96%	446.83	7.61%
51:52	E:F	391.10	393.22	-0.54%	0.08%	423.56	-7.66%
55:56	S:T	321.52	282.73	13.72%	2.06%	337.85	-4.83%
55:56	X:Y	377.00	329.32	14.48%	2.17%	375.09	0.51%
65:66	Z1:Z2	276.45	273.57	1.05%	0.16%	330.31	-16.31%
65:66	N:O	274.75	285.67	-3.82%	0.57%	340.26	-19.25%
65:66	F:G	229.78	236.95	-3.03%	0.45%	299.33	-23.24%
63:64	C:D	223.75	227.92	-1.83%	0.27%	291.47	-23.23%
61:62	B:C	183.02	199.05	-8.05%	1.21%	265.63	-31.10%
61:62	C:D	193.68	234.92	-17.55%	2.63%	297.57	-34.91%
63:64	Z2:Z3	403.33	393.87	2.40%	0.36%	424.04	-4.88%
56:57	Z2:Z3	368.67	339.45	8.61%	1.29%	382.95	-3.73%
38:39	Z2:Z3	220.48	216.84	1.68%	0.25%	281.68	-21.73%
68:69	M:N	326.30	371.45	-12.16%	1.82%	407.35	-19.90%
63:64	T:U	305.60	294.17	3.89%	0.58%	347.16	-11.97%
62:63	C:D	263.52	268.54	-1.87%	0.28%	326.14	-19.20%
58:59	M:N	220.20	203.81	8.04%	1.21%	269.96	-18.43%
70:71	N:O	280.22	299.74	-6.51%	0.98%	351.66	-20.31%
70:71	R:S	268.30	303.94	-11.73%	1.76%	355.03	-24.43%
63:64	X:Y	529.87	503.91	5.15%	0.77%	502.04	5.54%
63:64	U:V	523.00	494.53	5.76%	0.86%	495.62	5.52%
69:70	S:T	823.32	780.81	5.44%	0.82%	677.79	21.47%
68:69	E:F	777.67	727.45	6.90%	1.04%	645.69	20.44%
67:68	O:P	530.10	529.02	0.20%	0.03%	519.06	2.13%
70:71	O:P	815.30	856.10	-4.77%	0.71%	721.93	12.93%
70:71	B:C	897.30	848.89	5.70%	0.86%	717.76	25.01%
68:69	K:L	715.27	712.46	0.39%	0.06%	636.54	12.37%
69:70	X:Y	751.88	762.27	-1.36%	0.20%	666.72	12.77%
68:69	Z2:Z3	435.33	374.45	16.26%	2.44%	409.60	6.28%
64:65	B:C	132.03	140.89	-6.29%	0.94%	209.61	-37.01%
39:40	Z2:Z3	95.18	72.54	31.21%	4.68%	132.99	-28.43%
55:56	C:D	102.97	102.20	0.76%	0.11%	168.20	-38.78%
68:69	N:O	144.68	153.99	-6.04%	0.91%	222.77	-35.06%
68:69	Z2:Z3	175.53	179.37	-2.14%	0.32%	247.33	-29.03%
49:50	M:N	241.13	265.65	-9.23%	1.38%	323.73	-25.51%
58:59	R:S	32.50	30.93	5.07%	0.76%	74.15	-56.17%
56:57	R:S	32.62	31.03	5.11%	0.77%	74.31	-56.11%
65:66	R:S	24.18	31.32	-22.80%	3.42%	74.79	-67.67%
56:57	N:O	27.93	29.38	-4.93%	0.74%	71.58	-60.98%
47:48	N:O	21.62	22.55	-4.13%	0.62%	59.71	-63.79%
46:47	R:S	23.80	24.88	-4.36%	0.65%	63.88	-62.74%
44:45	T:U	31.82	29.00	9.72%	1.46%	70.94	-55.15%

40:41	C:D	30.32	29.48	2.84%	0.43%	71.74	-57.74%
51:52	T:U	33.67	28.24	19.23%	2.89%	69.66	-51.67%
51:52	Z2:Z3	37.55	32.53	15.42%	2.31%	76.76	-51.08%
53:54	B:C	42.83	43.63	-1.83%	0.27%	93.86	-54.37%
51:52	B:C	51.30	48.91	4.88%	0.73%	101.51	-49.46%

Using the power regression calibration, four comparisons are just outside the ±15% tolerance but within 20% and three others outside the 20% range. In these cases, a repeat measurement can be made at the location as well as surrounding locations to ascertain whether the comparison is outside the tolerance level. Figure 2 shows the calibrated predicted response versus the measured response. The linear fit shown in this figure indicates that the calibration used provides consistency between the predictions and measurements. Overall the average difference between the measured and predicted responses is 1.9%±9% which demonstrates that the calibration does not introduce a bias. In contrast, the use of a single linear regression calibration, results in very poor comparisons with thirty-six out of fifty-six falling outside the ±15% tolerance level.

Figure 2. Measured and Predicted Comparison Derived with Power Regression Calibration

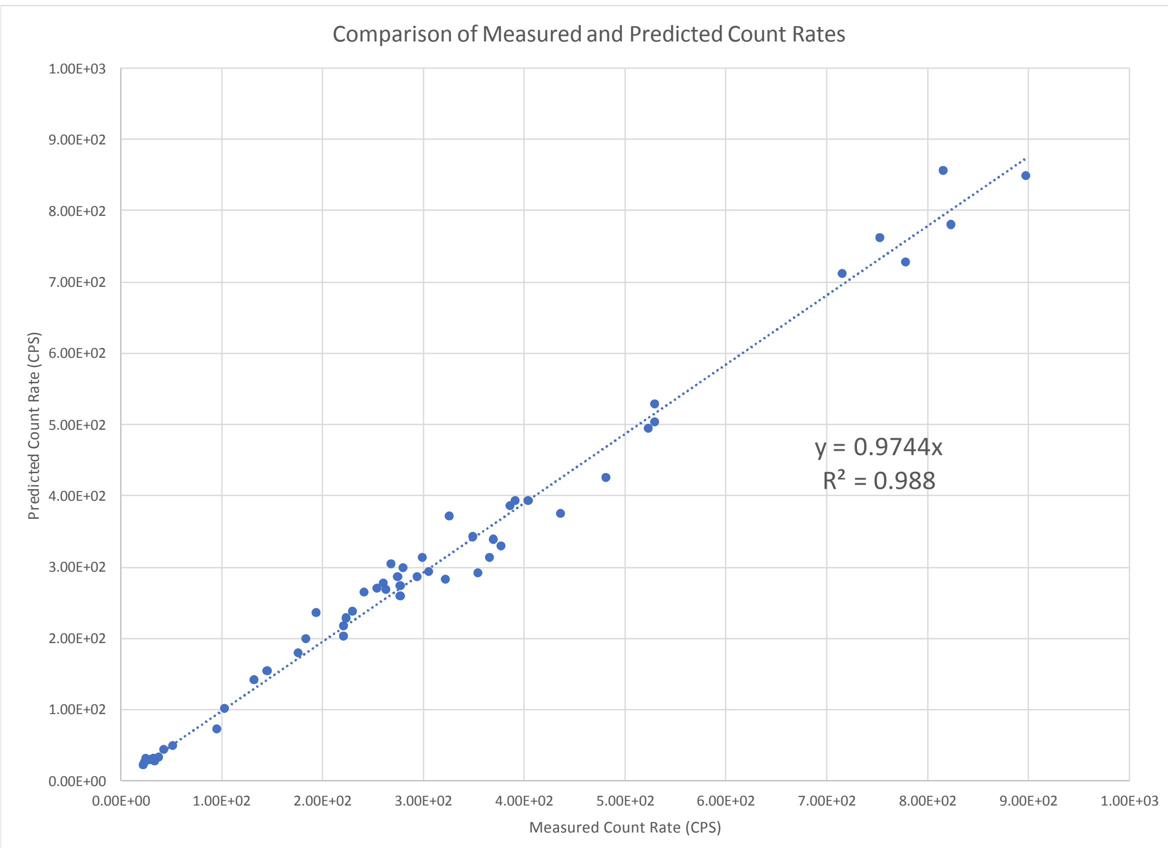

Detectability of Missing Fuel

The adequacy of the methodology using the power regression calibration on the predicted responses to detect a missing SFA from among the four nearest can be demonstrated by removing the SFA with the weakest signal from among the four. Since this was not possible during the field test, the comparison of the data that the software would predict with and without the weakest SFA can provide a good indication of the drop in the measured count rate. This was accomplished by removing that SFA from the Excel file that the software reads to populate the level. The removal of the SFA with the weakest signal among the four provides an indication of the limiting drop in the response that can be expected. Table 3 shows the drop in the predicted count rate when the SFA is removed. Like the responses presented in Table2, the predicted responses presented in Table 3 were also calculated by applying the power regression calibration to the uncalibrated responses from the software using spreadsheets.

Table3. Comparison of Count Rates with and without a Missing SFA

Position row	Position Column	Predicted-intact	Predicted-missing fuel	Percent difference ± uncertainty	
44:45	N:O	313.21	244.33	-21.99%	3.30%
44:45	K:L	313.21	238.52	-23.85%	3.58%
43:44	K:L	270.08	198.25	-26.60%	3.99%
38:39	H:J	286.46	227.90	-20.44%	3.07%
38:39	Q:R	292.18	229.12	-21.58%	3.24%
38:39	Z1:Z2	260.10	203.07	-21.92%	3.29%
44:45	X:Y	276.67	219.38	-20.71%	3.11%
51:52	V:W	341.94	258.61	-24.37%	3.66%
51:52	K:L	386.71	308.27	-20.28%	3.04%
57:58	H:J	425.13	328.98	-22.62%	3.39%
51:52	E:F	393.22	308.47	-21.55%	3.23%
55:56	S:T	282.73	215.83	-23.66%	3.55%
55:56	X:Y	329.32	244.37	-25.80%	3.87%
65:66	Z1:Z2	273.57	218.77	-20.03%	3.00%
65:66	N:O	285.67	188.71	-33.94%	5.09%
65:66	F:G	236.95	185.60	-21.67%	3.25%
63:64	C:D	227.92	177.38	-22.18%	3.33%
61:62	B:C	199.05	181.07	-9.03%	1.36%
61:62	C:D	234.92	212.29	-9.63%	1.45%
63:64	Z2:Z3	393.87	290.33	-26.29%	3.94%
56:57	Z2:Z3	339.45	255.36	-24.77%	3.72%
38:39	Z2:Z3	216.84	163.20	-24.74%	3.71%
68:69	M:N	371.45	293.62	-20.95%	3.14%
63:64	T:U	294.17	236.37	-19.65%	2.95%
62:63	C:D	268.54	210.07	-21.77%	3.27%
58:59	M:N	203.81	162.20	-20.42%	3.06%
70:71	N:O	299.74	233.36	-22.15%	3.32%
70:71	R:S	303.94	242.05	-20.36%	3.05%
63:64	X:Y	503.91	384.08	-23.78%	3.57%

63:64	U:V	494.53	395.42	-20.04%	3.01%
69:70	S:T	780.81	602.43	-22.85%	3.43%
68:69	E:F	727.45	575.02	-20.95%	3.14%
67:68	O:P	529.02	391.20	-26.05%	3.91%
70:71	O:P	856.10	676.40	-20.99%	3.15%
70:71	B:C	848.89	645.23	-23.99%	3.60%
68:69	K:L	712.46	560.13	-21.38%	3.21%
69:70	X:Y	762.27	597.14	-21.66%	3.25%
68:69	Z2:Z3	374.45	282.93	-24.44%	3.67%
64:65	B:C	140.89	123.65	-12.24%	1.84%
39:40	Z2:Z3	72.54	64.32	-11.34%	1.70%
55:56	C:D	102.20	93.04	-8.96%	1.34%
68:69	N:O	153.99	129.90	-15.64%	2.35%
68:69	Z2:Z3	179.37	161.56	-9.93%	1.49%
49:50	M:N	265.65	205.93	-22.48%	3.37%
58:59	R:S	30.93	21.30	-31.14%	4.67%
56:57	R:S	31.03	23.49	-24.31%	3.65%
65:66	R:S	31.32	23.78	-24.09%	3.61%
56;57	N:O	29.38	23.08	-21.44%	3.22%
47:48	N:O	22.55	16.89	-25.10%	3.76%
46:47	R:S	24.88	19.41	-22.01%	3.30%
44:45	T:U	29.00	22.57	-22.17%	3.33%
40:41	C:D	29.48	23.22	-21.22%	3.18%
51:52	T:U	28.24	22.21	-21.33%	3.20%
51:52	Z2:Z3	32.53	25.53	-21.54%	3.23%
53:54	B:C	43.63	33.57	-23.07%	3.46%
51:52	B:C	48.91	38.89	-20.49%	3.07%

The drop in signal exceeds the tolerance of 15% with an average of -22%±4.5%. There are some cases where the drop is below or very near 15%. In these cases, moving the measurement to an adjacent location can detect this missing fuel. Table 4 presents the data for four of these locations.

Table 4. Detectability of Missing SFAs by Using Adjacent Locations

Original Row	**Original Column**	**New Row**	**New Column**	**Count Rate without SFA**	**Count Rate with SFA**	**Difference± uncertainty**	
39:40	Z2:Z3	39:40	Z1:Z2	3.32E+01	3.99E+01	-16.9%	2.5%
55:56	C:D	55	C:D	1.66E+01	2.22E+01	-25.2%	3.7%
68:69	N:O	67:68	N:O	3.84E+01	4.79E+01	-19.9%	3.0%
68:69	Z2:Z3	67:68	Z1:Z2	4.51E+01	5.41E+01	-16.7%	2.5%

The differences for the four cases now exceeds the set tolerance. Three of the locations had drops in the -10-12% range. These were the cases where isolated NU SFAs were surrounded by SEU SFAs in Pool 4. The drop in the signal is lower than 15% in these cases. These locations were chosen for measurement to test the detectability limits of the tool. This rare scenario consisting of three locations among the over 4000 SFAs present in the upper level of the four pools may pose a challenge to detectability. If the randomly selected locations fall at the boundary of NU and SEU SFAs moving one slot above or below that would improve the detectability of a missing NU SFA with a weaker neutron signal.

Measurements in Pool 7

The SFAs in the upper level of pool 7 were left undisturbed since the last measurements were made in 2004. Measurements were made at four locations to determine the impact of an additional 12.5 years of cooling time on the count rates. All four data points showed a decline in the count rates compared to those recorded in 2004. This pool had large extraneous hardware from other pools stored over it thus preventing more measurements from being taken. The three NU SFAs locations registered drops of 13-25%, while the single location with newer SEU SFAs registered a smaller drop of 5% - a drop that is lower than expected.

Calibration of the Software

The new approach to calibrating the predicted count rate against the measured count rate with use of power law regression provides a single calibration set covering the entire range of count rates from the field test data. The current measurements were all made at the upper level in each pool with a close pack 123 x 150 mm inter-assembly pitch. The lower level consists of a mix of both 150 x150 and 123 x 135 mm pitches. The transfer functions used in the software accounts for these inter-assembly pitches and the calibration is likely to remain consistent with that developed in this study. However, when measurements are made in the lower level it is recommended that the calibration be done to ensure that it adequately represents these different pitches.

It is emphasized that the *current version of the software that was provided to ABACC in late 2015, does not contain the new calibration function* and *would need to be updated to include it* to make the software far more user friendly and easy to use for real time verification. More importantly, the software will contain an algorithm that is empirically representative of the behavior of the measured neutron signals from the SFAs.

Summary of the Results

The field test provided a good mix of data with a wide range of count rates that helped identify an issue with the current version of the software. The use of power function based calibration in lieu of the linear calibration currently used, enabled the development of one calibration set valid for the entire range of count rates recorded. The results presented in the previous sections indicate that with a power function-based calibration, the software predicts expected count rates regardless of cooling time or burnup and can also detect missing fuel at a measurement location in virtually all situations. The software would need to be updated to replace the old calibration with the new power function based one for it to be able to use a single calibration set and thus enable a more user-friendly real time verification process. The software, SFVT, coupled with the tool, SFNC, will provide a quantitative means of verifying the presence of spent fuel at the Atucha-1 site.

References

1. S. Sitaraman, Y. Ham, N. Gharibyan, O. Peixoto, and G. Diaz, “Methodology and Software for Gross Defect Detection of Spent Nuclear Fuel at the Atucha-1 Reactor”, *Nuclear Technology,* volume 92, pp 74-83, October 2015.
2. A. Carter, S. Sitaraman, N. Gharibyan, and Y. Ham, “Atucha-1 Spent Fuel Verification Tool-User’s Manual”, Revision 2, LLNL-SM-675981, August 2015.

Acknowledgements

The author wishes to thank the following for their invaluable contribution to the success of the field test campaign:

Young-Gil Lee and Yong-Sung Lee of the International Atomic Energy Agency

German Krause and Nestor Eilers of Nucleoelectrica Argentina S.A

Anibal Bonino and Luis Machado of ABACC

Gustavo Diaz and Vicente Garcia Fraga of ARN

Ruth Smith and Anthony Belian of the USDOE-INSEP

Philip Kerr of LLNL

The author also wishes to thank Narek Gharibyan and Austin Carter from LLNL for their help with the software development.

The author wishes to thank Young Ham of LLNL who originated this project and has provided guidance and support during its course.